Received: 1 July 2024 | Revised: 20 September 2024 | Accepted: 20 November 2024 | Published online: 27 November 2024

RESEARCH ARTICLE

Medinformatics
2024, Vol. 00(00) 1–12
DOI: 10.47852/bonviewMEDIN42023732

BON VIEW PUBLISHING

Computational Analysis to Identify Novel Drug Targets for Esophageal Cancer

Vinod Jangid[1,*], Chandrasekar Narayanan Rahul[2], Aarthi Rashmi B[1] and Kanagaraj Sekar[2]

[1]*Department of Bioinformatics, Sri Krishna Arts and Science College, India*

[2]*Department of Computational and Data Sciences, Indian Institute of Science, India*

Abstract: Cancer is a multigene and widespread disease. Increasing drug resistance leads to the development of new therapeutic targets. Recent research indicates that various cellular components called stress granules (SGs) are engaged in the cancer-related signaling pathway. The phosphoinositol-3-kinase (PI3K)/AKT/mammalian target of rapamycin (mTOR) signaling, considered a master regulator in cancer, has been shown through genomic profiling studies to play a key role in esophageal cancer (EC). In this study, we performed the in silico analysis of an RNA sequencing dataset to investigate the effects of omipalisib, a PI3K/mTOR inhibitor, on EC cell lines. Our objective was to identify novel molecular targets, particularly SG-related proteins, that contribute to drug resistance in EC. Using computational approaches including differential gene expression analysis, pathway analysis, and functional enrichment, we examined the transcriptomic changes in response to omipalisib treatment. Our analysis revealed downregulation of the PI3K/mTOR signaling pathway and upregulation of compensatory pathways such as FOXO and JAK-STAT signaling in response to omipalisib. Notably, we identified 16 SG-related proteins that were significantly upregulated, suggesting their potential role in drug resistance mechanisms. These findings provide new insights into the molecular mechanisms underlying drug resistance in EC and highlight potential novel targets for therapeutic intervention. Currently, EC is limited by the number of potential drugs for treatment and poor prognosis and is prone to chemotherapeutic resistance to existing clinically proven drugs. Our computational analysis offers valuable insights into targeting SGs for cancer drug discovery, potentially enhancing the development of new therapeutic strategies for EC. These results provide a strong foundation for future experimental validation and drug development efforts aimed at overcoming resistance to EC treatment.

Keywords: esophageal cancer, drug resistance, RNA-seq, PI3K/AKT/mTOR, stress granules, FOXO, JAK-STAT

1. Introduction

Esophageal Cancer (EC) is the seventh most common malignancy among all the known cancer types worldwide. With approximately 500,000 new cases reported annually, EC ranks sixth in terms of mortality, with a poor 5-year survival rate [1]. Adenocarcinoma and squamous cell carcinoma are the two subtypes of EC. The status of EC indicates it to be one of the various well-studied cancers with no known curative treatment. Current standard therapies rely on surgery, chemotherapy, and radiotherapy, highlighting the urgent need for newer strategies and approaches to overcome drug resistance.

A central challenge in EC treatment is the development of drug resistance, which significantly limits the long-term efficacy of current therapies. Aberrant activation of the phosphatidylinositol 3 kinase pathway or PI3K pathway has been widely implicated in many cancers, and increased activity of this pathway is often implicated in resistance to cancer therapies [2]. This underscores the urgent need for novel molecular targets that could lead to more effective treatment strategies. The phosphoinositol-3-kinase (PI3K)/AKT/mammalian target of rapamycin (mTOR) signaling pathway is a central regulator of cancer cell growth, survival, and metabolism [3]. PI3K is a plasma membrane-associated lipid kinase that, upon activation by growth factors or other extracellular signals, initiates a cascade leading to the activation of AKT and mTOR. Inhibitors targeting PI3K and mTOR, such as omipalisib, have shown potential in preclinical studies by disrupting critical signaling networks in cancer cells. However, despite initial efficacy, cancer cells often develop resistance to these inhibitors, limiting their long-term therapeutic benefits [4].

Inhibitors targeting PI3K and mTOR, such as omipalisib, have shown promise in preclinical studies by disrupting critical signaling networks in cancer cells. Omipalisib, a member of the quinolines, is an ATP-competitive inhibitor that has sub-nanomolar action on p110α, p110β, p110γ, and p110δ, as well as the mTOR1 and mTOR2 complexes [5]. It inhibits PI3K in the PI3K/mTOR signaling pathway and thus triggers apoptotic cell death [6]. Recent studies support the rationale for using omipalisib as a therapeutic approach for ESCC patients [3]. However, despite initial efficacy, cancer cells often develop resistance to these inhibitors, limiting their long-term therapeutic benefits [4].

The complexity of the PI3K/AKT/mTOR signaling network is substantial, and recent studies suggest several possible resistance mechanisms. One of the less explored resistance mechanisms in

*Corresponding author: Vinod Jangid, Department of Bioinformatics, Sri Krishna Arts and Science College, India. Email: vinodjangid.jdr@gmail.com

ES is the involvement of stress granules (SGs) that is linked to the PI3K pathway. SGs are a type of membrane-less organelle that arise when cells are exposed to stress stimuli and help the cells cope with the stress [7]. Their formation is critical for cell survival because these block apoptosis by reducing reactive oxygen species, sequestering signaling molecules, and stabilizing anti-apoptotic factor mRNAs [8]. When translation initiation is halted, SGs form in the cytoplasm and contain RNA-binding proteins, non translated RNAs, several types of translation initiation factors, poly(A)-binding proteins, and ribosomal subunits [9]. When stresses are encountered, SGs instantly assemble and are cleaned up once the stressors have passed [10]. Cancer cells exist in a complex microenvironment that is characterized by high-stress stimuli like oxidative stress, ER stress, hypoxia, and nutrient deprivation [11].

In the present study, we perform in silico analysis of an RNA sequencing dataset obtained from an ESCC cell line in response to omipalisib treatment. Our primary objective is to identify novel molecular targets, specifically SG-related proteins, which contribute to drug resistance in EC. We hypothesize the existence of integrated stress response upon omipalisib drug action. We infer from our analysis that novel molecular targets could serve as strong predictors of poor prognosis and serve to be key targets for further drug discovery against EC. By identifying these targets, we also propose novel therapeutic strategies that could enhance the effectiveness of PI3K/AKT/mTOR inhibitors in EC treatment.

2. Materials and Methods

The Gene Expression Omnibus (GEO) database was searched for gene expression profiling studies related to drug resistance in EC. Following a thorough review of the literature, we identified that a study on the RNA sequencing dataset of esophageal tumor cell line "KYSE150" (GEO_Accession "GSE143462") is most suitable to examine our hypothesis. Thus, we used this dataset for computational analysis to gain further insights into novel molecular targets for EC discovery [3].

The methodology adopted in the present study involves various tools in a stepwise manner. The tools mainly include the Short Read Archive (SRA) tool kit [12], RNASTAR [13], FASTQC [14], MultiQC [15], RSeQC [16], Feature Counts [17], and DESeq2 [18]. They represent a pipeline for analysis of the RNA sequences for gene expression study of a specific cancer type. These tools are present as a collection in the web-based platform called RNA Galaxy suite. To utilize the above bioinformatics tool to its maximum potential, we initially tried to optimize the usage of each tool in the galaxy suite [19].

2.1. Differential gene expression analysis

GEO [20], a repository that contains microarray, next generation sequencing, and other technologies, is archived and publicly distributed datasets, used to analyze RNA-seq data from esophageal tumor cell line "KYSE150" with two condition control and treated with omipalisib (Table 1). Downloaded all fastq files from the SRA data from the National Center for Biotechnology Information (NCBI) using SRA toolkit-2.11.0 [12] after uploading the accession number text file on Galaxy suite. The FastQC-0.11.8 [14] and MultiQC-1.11 [15] tools were used to analyze the quality of the RNA-seq reads, and they were aligned to the GRCh38 reference genome using the STAR-2.78a tool [13]. STAR (Spliced Transcripts Alignment to a Reference) is an RNA-seq read mapper that uses suffix arrays, seed clustering, and stitching algorithms to locate and map noncanonical splice sites, chimera sequences, and full-length RNA sequences. RSeQC-2.6.4 [16] was used to assess the quality of BAM files, featureConts-2.0.1 [17] was used to quantify the transcripts, and the DESeq2-1.34.0 [18] program was used to find differentially expressed genes.

2.2. Functional enrichment analysis

PathView web tool produces significant, hyperlinked pathway graphs and allows for simple interactive access. PathView, a Bioconductor package, was used to check if the genes detected have a specific role in a pathway [21].

2.3. EGSEA

The ensemble of gene set enrichment analyses (EGSEA) is a technique for RNA sequencing data that integrates the outcomes of 12 algorithms and produces collective gene set scores to increase the biological relevance of the top-ranked gene sets. An input of a count's matrix (counts table) containing raw RNA-seq read counts was used to generate outputs in various formats like Stats table, Heatmap, Summary plots, Pathways, and GO (Gene Ontology) graph [22]. GOseq was used to investigate the biological functions of major differentially expressed genes in the study using gene ontology enrichment analysis. It is evaluated with the Wallenius *P*-value with the Benjamini-Hochberg-corrected *P*-value default program [23].

3. Results

3.1. In silico analysis of transcriptome profiles in response to omipalisib treatment

Examination of transcriptome profile in response to omipalisib-treated "KYSE150" cell lines indicated that a total of 10003 genes were differentially expressed. The highly upregulated gene with the lowest *p* value of 5.91e-132 was MMPIO at 5.28 log2(FC) whereas the highly downregulated gene with the lowest *p*-value of 5.48e-18 was CHACl at −3.19 log2(FC).

Table 1. The properties of the RNA-seq datasets used in this study

GEO_Accession	Source_name	Treatment
GSM4259875	KYSE150 is not treated by omipalisib	Control
GSM4259876	KYSE150 is not treated by omipalisib (repeated)	Control
GSM4259877	KYSE150 is not treated by omipalisib (repeated)	Control
GSM4259878	KYSE150 is treated by omipalisib	Omipalisib
GSM4259879	KYSE150 is treated by omipalisib (repeated)	Omipalisib
GSM4259880	KYSE150 is treated by omipalisib (repeated)	Omipalisib

Figure 1. Principal component analysis. A variation of 5% across sample clusters is acceptable, and a variance of 92% between experiment conditions is expected.

3.2. Quality control and differential expression analysis

Sample-level quality check by principal component analysis assures that how well do our replicates cluster together? and whether experimental conditions represent the major source of variation. We obtained an acceptable score showing the experimental condition variance (PCl > 90%) and within-sample variance (PC2 < 5%) (Figure 1). MA plot visualizes and identifies gene expression changes from two different conditions. Genes with similar expression values in both normal and treated samples will cluster around the M = O value, i.e., no significant difference, the gene is upregulated when M > O, and it is downregulated when M < 0 (Figure 2). There are 2,522 upregulated genes (log2(FC) > 0; *p*-value 0.5) and 3036 downregulated genes (log2(FC) < 0; *p*-value 0.5 found after DESeq2-output analysis. Table 2 lists the differentially expressed genes that have been significantly upregulated and downregulated.

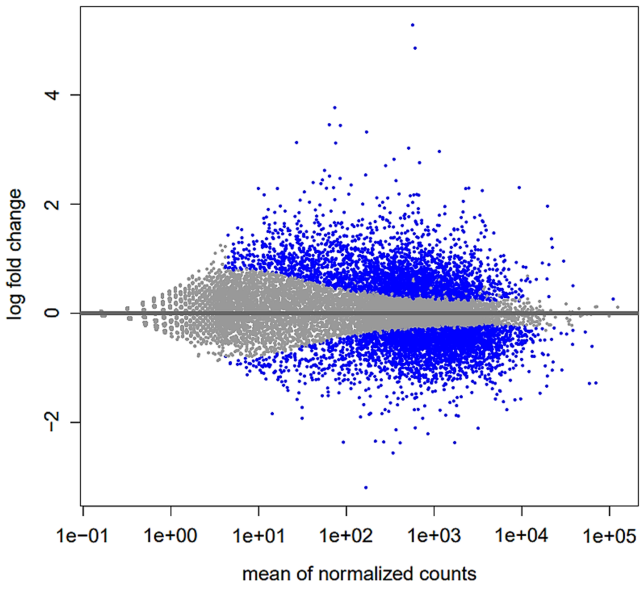

Figure 2. MA-d for Drug: resistant vs sensitive: Downregulated genes are more than upregulated. M = 0: significant difference, M > 0: gene is upregulated, M < 0: gene is downregulated

3.3. Pathway analysis and functional enrichment

We performed comprehensive pathway analysis and functional enrichment to move beyond the simple cataloging of differentially expressed genes. Functional enrichment analysis using Pathview indicates the mTOR signaling pathway to be the most downregulated (Figure 3). According to previous research, omipalisib therapy disrupted the activation of PI3K/AKT/mTOR and ERK signaling by decreasing the expression of p-AKT, p-4EBP1, p-p70S6K, p-S6, and p-ERK [3]. This result is re-established in the present analysis. Apart from mTOR signaling, we observed the FOXO signaling pathway upregulated (Figure 4), and the JAK-STAT signaling upregulated (Figure 5). As shown in Table 3, most genes were likewise discovered to be downregulated and upregulated associated with their pathway with log2(FC) and *p*-value.

Table 2. Topmost significantly upregulated and downregulated differentially expressed genes

Upregulated			
Gene ID	Gene symbol	Log2(FC)	P-adj
4319	MMP10	5.280233	$4.10e^{-133}$
4322	MMP13	4.858445	$2.98e^{-148}$
4321	MMP12	3.767515	$7.57e^{-33}$
284029	LINC00324	3.454341	$3.19e^{-27}$
8743	TNFSF10	3.441384	$4.09e^{-26}$
9976	CLEC2B	3.321622	$2.73e^{-47}$
1003	CDH5	3.127903	$2.28e^{-15}$
4314	MMP3	3.119116	$1.56e^{-26}$
3433	IFIT2	3.026504	$5.25e^{-15}$
114907	FBXO32	2.964443	$3.52e^{-111}$
Downregulated			
Gene ID	Gene symbol	Log2(FC)	P-adj
79094	CHAC1	−3.19259	$2.88e^{-16}$
57103	TIGAR	−2.55906	$1.54e^{-41}$
57026	PDXP	−2.37463	$9.23e^{-36}$
29968	PSAT1	−2.37042	$4.96e^{-53}$
84915	FAM222A	−2.3621	$1.86e^{-17}$
25907	TMEM158	−2.35788	$2.76e^{-25}$
8862	APLN	−2.34395	$6.44e^{-24}$
993	CDC25A	−2.2083	$3.88e^{-44}$
122953	JDP2	−2.13486	$3.05e^{-26}$
595	CCND1	−2.107	$6.15e^{-30}$

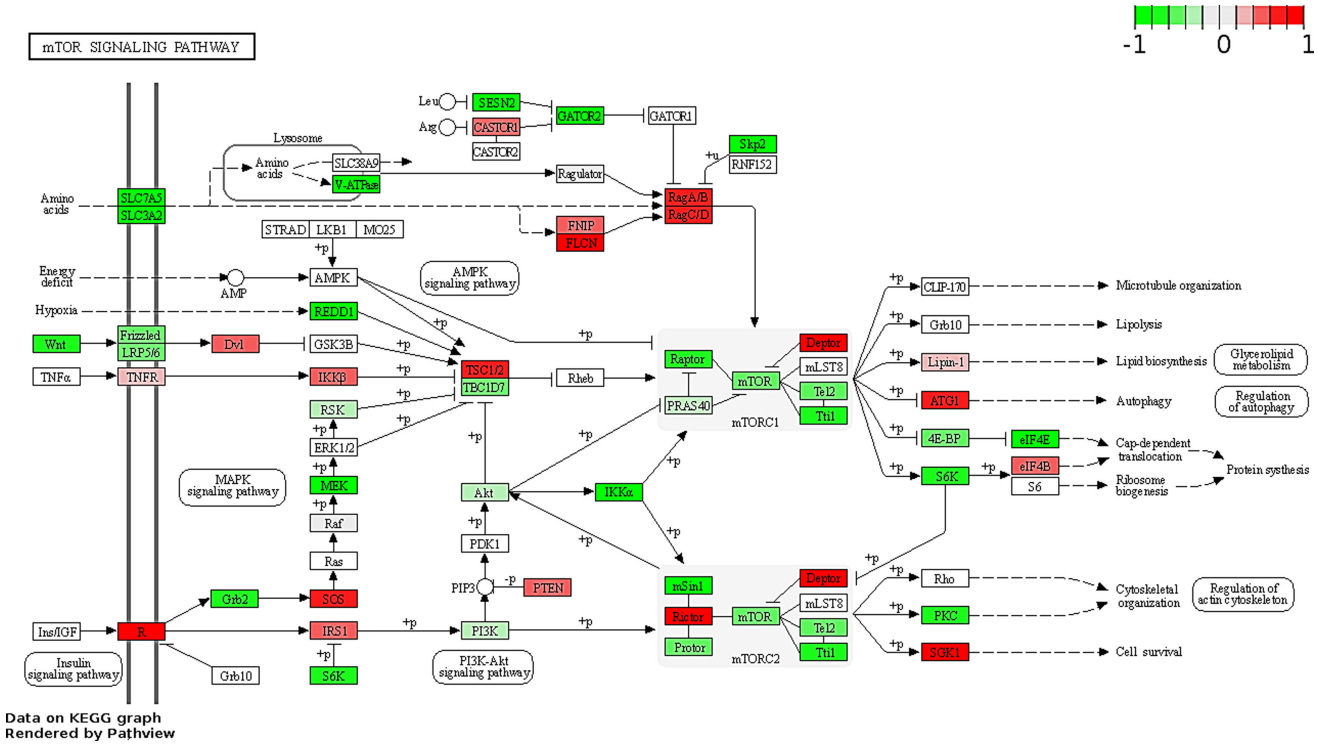

Figure 3. "mTOR signaling pathway" Upregulated genes are labeled red, whereas downregulated genes are colored green.

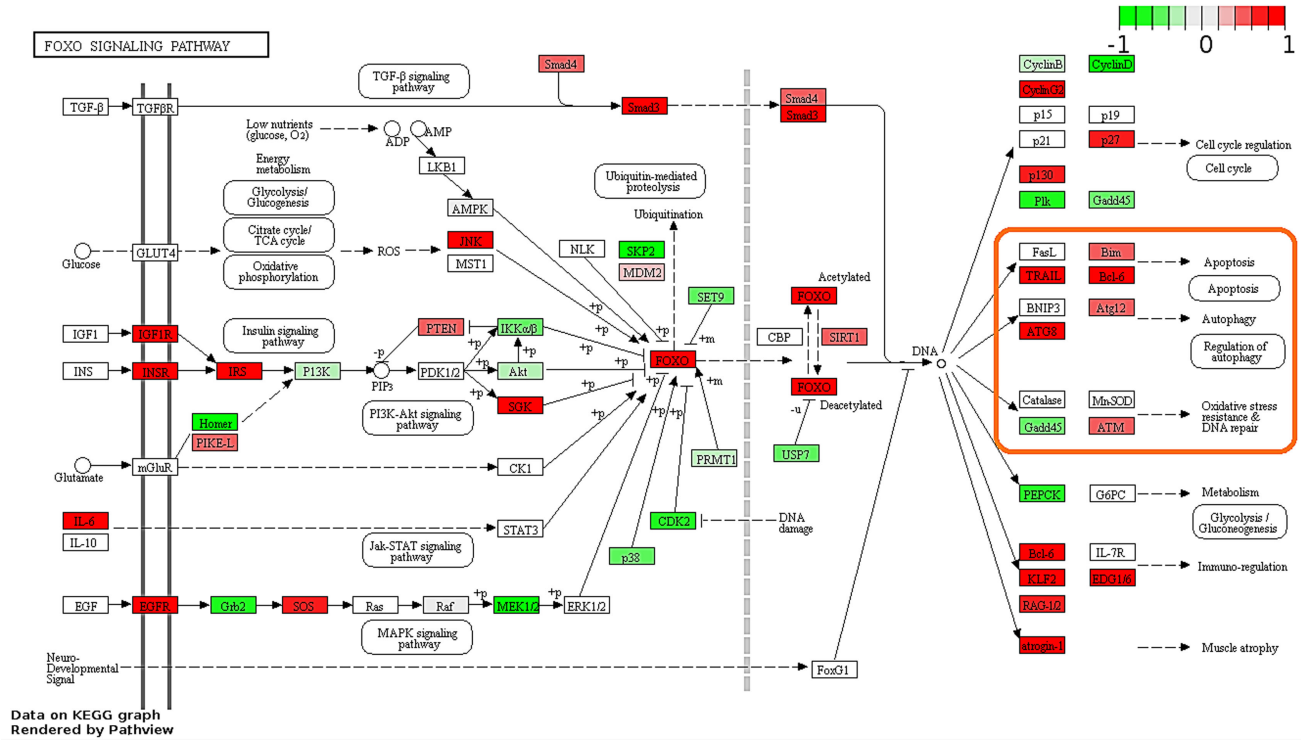

Figure 4. "FoxO signaling pathway" Upregulated genes are labeled red, whereas downregulated genes are colored green. In the orange box, the main genes are featured along with their notable works.

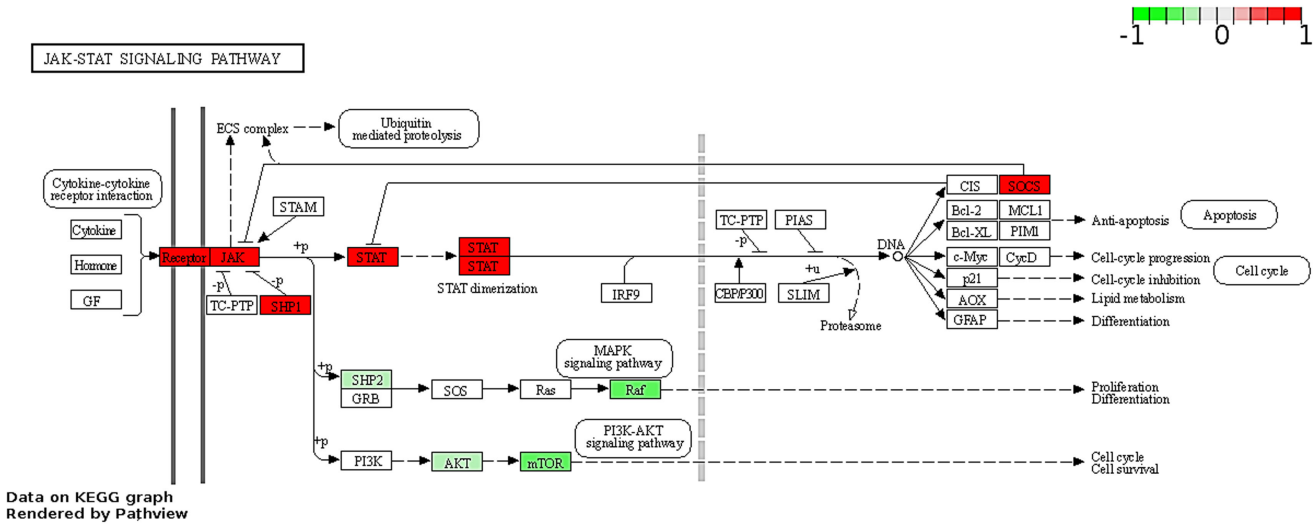

Figure 5. "JAK-STAT signaling pathway" Upregulated genes are labeled red, whereas downregulated genes are colored green.

Table 3. Major pathway and their most significant enriched genes

mTOR signaling pathway			
GeneID	Gene	Log(2)FC	*P*-value
207	AKT1	−0.3654	$2.08e^{-03}$
2475	mTOR	−0.4874	$1.1e^{-04}$
9894	TELO2	−0.5489	$5.74e^{-06}$
9675	TTI1	−0.7326	$2.66e^{-11}$
1978	EIF4EBP1 (4E-BP1)	−0.4348	$4.08e^{-04}$
6199	RPS6KB2 (S6K)	−0.6800	$2.07e^{-08}$
1977	EIF4E	−0.9605	$2.86e^{-07}$
9470	EIF4E2	−0.4403	$6.27e^{-05}$
FoxO signaling pathway			
GeneID	Gene	Log(2)FC	*P*-value
2308	FOXO1	0.71007	$1.12e^{-06}$
2309	FOXO3	0.38522	$4.075e^{-03}$
4303	FOXO4	1.16406	$1.48e^{-15}$
23411	SIRT1	0.48297	$1.97e^{-03}$
8743	TNFSF10 (TRAIL)	3.44138	$2.27e^{-28}$
23710	GABARAPL1 (ATG8)	2.28403	$7.56e^{-59}$
10018	BCL2L11 (BIM)	0.54143	$1.134e^{-04}$
604	BCL6	0.77408	$7.99e^{-05}$
9140	ATG12	0.44031	$5.516e^{-03}$
472	ATM	0.57146	$5.54e^{-05}$
JAK-STAT signaling pathway			
GeneID	Gene	Log(2)FC	*P*-value
3718	JAK3	1.55169	$4.75e^{-08}$
6773	STAT2	1.05548	$1.02e^{-15}$
6778	STAT6	0.76726	$7.08e^{-10}$
9021	SOCS3	1.524316	$1.08e^{-15}$

3.4. Gene set enrichment and ontology analysis

To further elucidate the biological significance of the observed gene expression changes, we conducted EGSEA and GOseq analyses. EGSEA functional enrichment analysis indicated that the hallmark cancer gene set TNFA_signalling_via_NFKB and KEGG pathway gene set FOXO signaling pathway was observed to be upregulated in response to the drug omipalisib. GOseq functional analysis results indicate enrichment of gene ontology terms related to RNA binding, mitochondria, and translation termination. Both EGSEA and Goseq analysis led us to examine further the involvement of SGs in response to the drug omipalisib.

3.5. Identification of novel SG-related proteins

Through our post-expression data mining, we observed the enrichment of sixteen novel proteins involved in SG's function that are found to be highly upregulated with log2(FC) > 1, and significant (P-adj < 0.05) and interpreted based on MSGP database r271 as shown in (Table 4, Figure 6). The findings of this study provide important insights into the molecular mechanisms underlying drug resistance in EC. By performing a detailed in silico analysis of RNA sequencing data from omipalisib-treated EC cell lines, we identified key molecular targets and pathways that may play crucial roles in mediating resistance to PI3K/mTOR inhibition.

4. Discussion

The current research problem in cancer therapeutics is about overcoming drug resistance. Studies on omipalisib are proven to surmount this resistance to a certain extent when used as a dual inhibitor of PI3K and mTOR signaling. Omipalisib is a dual inhibitor medication, which means it has two inhibitory actions. It is an ATP-competitive inhibitor with sub-nanomolar action against p110α, p110β, p110γ, and p110δ, as well as the mTOR1 and mTOR2 complexes [5]. However, a recent review [10] suggests that a chemotherapeutic resistance is conferred also in the case of such dual inhibitors like omipalisib in response to PI3K signaling pathway inhibition. This is reasoned, due to the complexity of the PI3K/AKT/mTOR signaling network which involves numerous feedback loops, extensive crosstalk nodes with other signaling pathways, and compensatory pathways, providing ample opportunities for circumventing the effects of PI3K inhibition [10].

Table 4. Highly unregulated stress granules

S. No	GeneID	log2fc	Adjusted P-value	Description	Remark	Reference
1.	ACAPI	1.20	7.44e-08	ArfGAP With Coiled-Coil, Ankyrin Repeat and PH Domains 1	l) ACAP expression is suggested to predict poor prognosis. 2) Expression and methylation strongly correlated with immune infiltration, regulated tumor microenvironment, and cancer cell sternness.	[24]
2.	ANG	1.00	0.002413	Angiogenin	1) Activate tumor angiogenesis. 2) ANG upregulation is associated with metastasis in colorectal cancer patients.	[25]
3.	DDX58	1.05	0.021888	DExD/H-Box Helicase 58	Immune surveillance protein is suggested to have a role in activating autophagy and protection from lipotoxicity. The study indicates the regulation of the autophagy receptor protein SQSTM1/p62 through DDX58. Activated DDX58 increases a cytoprotective autophagic response via SQSTM1/p62 and this aids cell survival in prostate cancer.	[26, 27]
4.	DST	2.26	$4.43e^{-30}$	Dystonia	Dystonia maintains focal adhesion integrity. DST isoform promotes migration, invasion, and tumorigenic potential in oral squamous carcinoma cells.	[28]
5.	DTX3L	1.25	$7.64e^{-19}$	E3 ubiquitin-protein ligase DTX3L	Deltex-3-like (DTX3L), also known as B-lymphoma and BAL-associated protein (BBAP), has been reported to play an important role in the progression of many tumors. DTX3L is reported to be highly expressed in the glioma tissues and its level was correlated with the grade of malignancy. Silencing of DTX3L improved sensitivity to chemotherapy drugs in multiple myeloma cell lines.	[29, 30]
6.	EIF4E3	1.41	$3.68e^{-08}$	Eukaryotic Translation Initiation Factor 4E Family Member 3	A family of translation initiation factors that bind to mRNA 5' cap regulating the proteome and cellular phenotype. EIF4E3 is suggested to act as the second branch of integrated stress response reprograming the translatome to promote stress resistance and adaptation.	[31, 32]
7.	GRB7	2.26	$1.36e^{-44}$	Growth Factor Receptor Bound Protein 7	An RNA-binding translation regulator. Regulates the dynamics of SG formation and assembly. GRB7 plays a role in regulating angiogenesis in ovarian cancer. GRB7 is reported to be an oncogenic driver in esophageal adenocarcinoma and a potential therapeutic target.	[33–35]
8.	IGF2BP3	1.10	0.000202	Insulin-like Growth Factor 2 mRNA-Binding Protein 3	Component of RNA granules. Implicated to establish a complex positive feedback loop that further facilitates tumor cell growth and malignancy.	[36]
9.	KIF13B	1.08	$1.91e^{-13}$	Kinesin Family Member 13B	The Kinesin superfamily is involved in different types of cancer. They are implicated in Triple Negative Breast Cancer proliferation and metastasis.	[37]
10.	OASL	1.43	0.002068	2'-5'-0ligoadenylate Synthetase Like	Studies suggest suppression of OASLI showed a synergistic effect on tumor clearance with conventional cancer therapies.	[38]

(*Continued*)

Table 4. (*Continued*)

S. No	GeneID	log2fc	Adjusted P-value	Description	Remark	Reference
11.	PARP14	1.32	$2.21e^{-13}$	Poly (ADP-Ribose) Polymerase Family Member 14	PARPl 4 is an interferon-stimulated gene (ISG) that is overexpressed in tumors compared to normal tissues and has been implicated by genetic knockout studies to promote pro-tumor macrophage polarization and suppress antitumor inflammatory response due to its role in modulating IL-4 and IFN-y signaling pathways. Current literature considers PARPI 4 as an intriguing drug target for the treatment of tumors and allergic inflammation. Utilizes nicotinamide adenine dinucleotide (NAD+) as a substrate to perform mono- or poly-ADP-ribosylation modification on target proteins	[39]
12.	PDCD4	1.50	$3.4e^{-20}$	Programmed Cell Death 4	Involved in the SG formation through its RNA-binding activity. It is suggested to be a potential target for mitigating SG-associated stress responses in obesity and related disease.	[40]
13.	SERPIN El	1.32	$6.2e^{-17}$	Serpine Family E Member 1	Upregulated in different types of cancer including oral squamous cell carcinoma. It is the cancer-promoting gene in gastric adenocarcinoma that facilitate tumor cell proliferation, migration, invasion, and regulating EMT. A high expression of these proteins increases drug resistance.	[41]
14.	SQSTMI	1.33	$4.62e^{-26}$	Sequestosome 1	A multifunctional adaptor protein implicated in selective autophagy, cell signaling pathways, and tumorigenesis.	[27, 28]
15.	TNKS	1.03	$1.95e^{-12}$	Tankyrase	Tankyrase, a member of the poly(ADP-ribose)polymerase family, mediates Wnt signal transduction and has emerged as a new molecular target for the therapy of different kinds of cancer. It also catalyzes ADP ribosylation of the target protein by moving a unit of ADP-ribose moiety from the NAD+ co-substrate.	[42]
16.	UPF3B	1.01	5.94E-07	UPF3B, Regulator of Nonsense Mediated mRNA Decay	Tumors adjust NMD activity to adapt to their microenvironment. Although they are suggested to play a complex role in cancer. Current literature considers PARPI 4 as an intriguing drug target for the treatment of tumors and allergic inflammation. Utilizes nicotinamide adenine dinucleotide (NAD +) as a substrate to perform mono- or poly-ADP-ribosylation modification on target proteins.	[43]

4.1. Novel insights into resistance mechanisms

In the present study, we used RNA sequencing-based computational analysis to provide insight into the association of SG participants with previously dealt PB-Kinase pathway. Upon computing differential gene expression using RNA-seq data and interpreting the gene list, we discovered interesting pathways. We observed the FoxO signaling pathway upregulated in response to resistance to oxidative stress [44] and the JAK-STAT signaling pathway upregulated in response to tissue stress [45] in response to omipalisib drug action. In the FoxO signaling pathway, the most upregulated genes are TNFSFIO, GABARAPLI, and FOX04 with log2(FC) 3.44138, 2.28403, and 1.16406 respectively and in the JAK-STAT signaling pathway most upregulated genes JAK3, SOCS3, and STAT2 with 1.55169, 1.524316, and 1.05548.

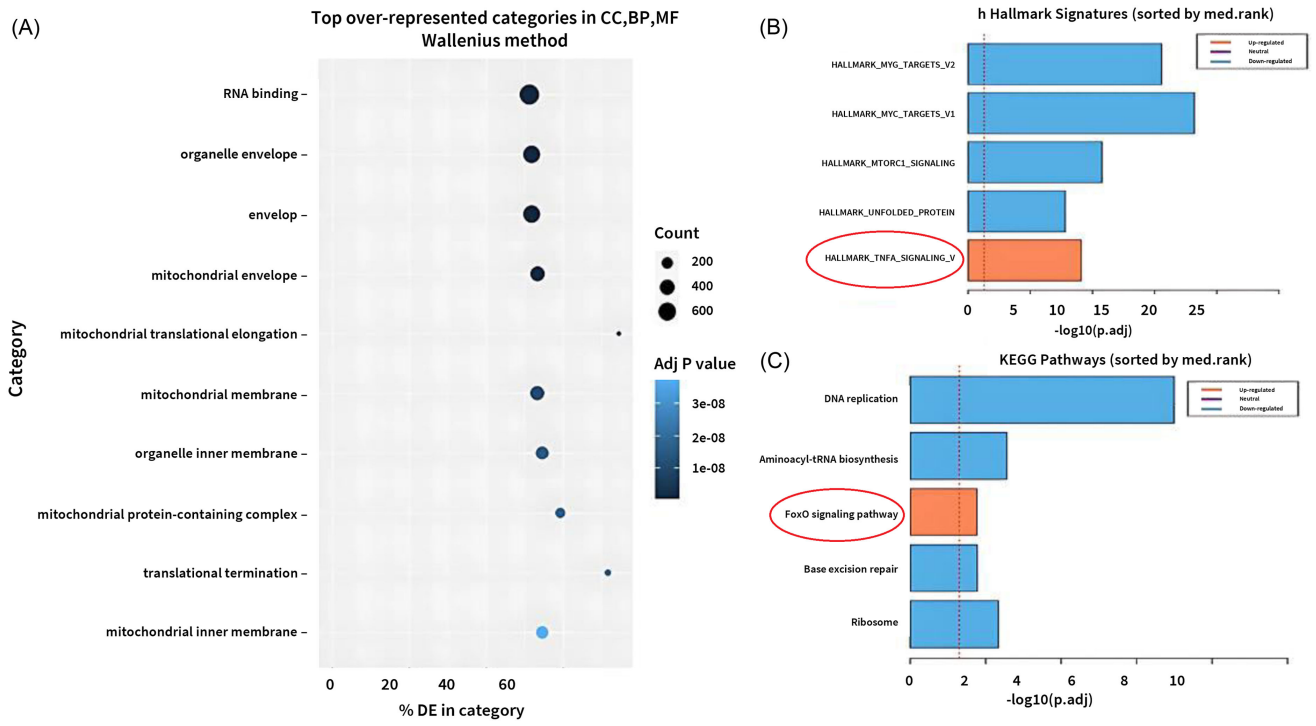

Figure 6. Functional enrichment analysis. (A) Goseq result represents top overrepresented functional categories. (B) & (C) EGSEA result representing summary plots of upregulated pathways highlighted in red circles

Based on the analysis of pathways enrichment results, we understand that the EC cell lines are subject to oxidative stress and tissue stress in response to omipalisib treatment. We further observed that a total of 16 proteins were highly expressed in response to omipalisib. They are implicated in the regulation and dynamics of SG assembly. Further, a detailed examination of these proteins (Table 4) supports the role of these SGs in promoting carcinogenesis and tumor growth. These results from our analysis are novel findings in the present study, and we report them to be useful therapeutic targets for further drug discovery and development of prognostic markers for EC treatment.

4.2. Autophagy and SGs in drug resistance

An earlier study on the omipalisib drug response to the EC cell line did not identify any role of autophagic response [3]. However, in our analysis, we find evidence for the role of autophagy. The signaling pathways reported in our analysis support the role of autophagy. In addition, the evaluation of SGs like DDX58 and SQSTMl plays a role in selective and cytoprotective autophagy response resulting in promoting tumorigenesis (Table 4). These results support the role of these SGs in promoting features like epithelial-mesenchymal transition (EMT), cancer cell sternness, and immune infiltration that are resultant due to adaptation to stress resistance under drug response and would lead to tumor growth and malignancy.

4.3. Corroboration with previous studies

Our results corroborate with earlier reports on the drug resistance to PI3K/AKT inhibition in the following ways: (a) Dual inhibition of PI3K and mTOR has been found to elicit a positive feedback response and lead to increased activation of JAK2/STAT5 and secretion of IL-8, thus contributing to drug resistance [46]. (b) The IL-6-STAT3 loop is suggested to trigger EMT [47]. The IL6 and STAT components are found to be upregulated in our computational analysis. This correlates with studies that show that EMT allows solid tumors to become more malignant, increasing their invasiveness and metastatic activity [48]. Hence, we suggest that the components of these pathways are differentially expressed to counteract the response to omipalisib drug action. Resistance to oxidative stress and tissue stress is highlighted in these pathways. This contributes to anti-apoptotic and cell survival features in cancer cells enhancing tumorigenesis in addition to emerging drug resistance.

4.4. Future directions and limitations

While our in silico analysis has revealed promising targets and pathways involved in drug resistance, it is important to note that these findings require experimental validation. Future studies should focus on validating the role of the identified SG-related proteins and signaling pathways through functional assays, such as knockdown or overexpression studies, and their impact on drug sensitivity in EC cell lines and patient-derived xenografts.

5. Conclusion

In conclusion, the association of the signaling pathways such as FoxO and JAK-STAT signaling observed in response to the omipalisib drug is a novel finding in our study. Further insight into the association of these pathways with SG formation is required to validate these new molecular targets and support drug design and discovery for the curative treatment of EC. Our study provides a strong foundation for future experimental work aimed at overcoming drug resistance in EC treatment.

Acknowledgement

The authors would like to thank the Laboratory for Structural Biology and Bio-computing, Department of Computational and Data Sciences, Indian Institute of Science, Bangalore, India, for providing complete support to execute this work.

Ethical Statement

This study does not contain any studies with human or animal subjects performed by any of the authors.

Conflicts of Interest

The authors declare that they have no conflicts of interest to this work.

Data Availability Statement

The data that support the findings of this study are openly available in the NCBI Gene Expression Omnibus (GEO) database under accession number GSE143462 at https://www.ncbi.nlm.nih.gov/geo/query/acc.cgi?acc=GSE143462.

Author Contribution Statement

Vinod Jangid: Conceptualization, Methodology, Software, Validation, Formal analysis, Data curation, Writing – original draft, Visualization. **Chandrasekar Narayanan Rahul:** Conceptualization, Methodology, Validation, Investigation, Writing – original draft. **Aarthi Rashmi B:** Validation, Writing – review & editing. **Kanagaraj Sekar:** Validation, Writing – review & editing, Supervision, Project administration.

References

[1] Huang, J., Koulaouzidis, A., Marlicz, W., Lok, V., Chu, C., Ngai, C. H., . . . , & Wong, M. C. S. (2021). Global burden, risk factors, and trends of esophageal cancer: An analysis of cancer registries from 48 countries. *Cancers*, *13*(1), 141. https://doi.org/10.3390/cancers13010141

[2] Millis, S. Z., Jardim, D. L., Albacker, L., Ross, J. S., Miller, V. A., Ali, S. M., & Kurzrock, R. (2019). Phosphatidylinositol 3-kinase pathway genomic alterations in 60,991 diverse solid tumors informs targeted therapy opportunities. *Cancer*, *125*(7), 1185–1199. https://doi.org/10.1002/cncr.31921

[3] Zhu, D. S., Dong, J. Y., Xu, Y. Y., Zhang, X. T., Fu, S. B., & Liu, W. (2020). Omipalisib inhibits esophageal squamous cell carcinoma growth through inactivation of phosphoinositide 3-Kinase (PI3K)/AKT/Mammalian target of rapamycin (mTOR) and ERK signaling. *Medical Science Monitor*, *26*, e927106. https://doi.org/10.12659/MSM.927106

[4] Liang, X., Chen, R., Wang, C., Wang, Y., & Zhang, J. (2024). Targeting HSP90 for cancer therapy: current progress and emerging prospects. *Journal of Medicinal Chemistry*, *67*(18), 15968–15995. https://pubs.acs.org/doi/10.1021/acs.jmedchem.4c00966

[5] Knight, S. D., Adams, N. D., Burgess, J. L., Chaudhari, A. M., Darcy, M. G., Donatelli, C. A., . . . , & Dhanak, D. (2010). Discovery of GSK2126458, a highly potent inhibitor of PI3K and the mammalian target of rapamycin. *ACS Medicinal Chemistry Letters*, *1*(1), 39–43. https://doi.org/10.1021/ml900028r

[6] Vachhani, P., Bose, P., Rahmani, M., & Grant, S. (2014). Rational combination of dual PI3K/mTOR blockade and Bcl-2/-xL inhibition in AML. *Physiological Genomics*, *46*(13), 448–456. https://doi.org/10.1152/physiolgenomics.00173.2013

[7] Riggs, C. L., Kedersha, N., Ivanov, P., & Anderson, P. (2020). Mammalian stress granules and P bodies at a glance. *Journal of Cell Science*, *133*(16), jcs242487. https://doi.org/10.1242/jcs.242487

[8] Gareau, C., Fournier, M. J., Filion, C., Coudert, L., Martel, D., Labelle, Y., & Mazroui, R. (2011). $p21^{WAF1/CIP1}$ upregulation through the stress granule-associated protein CUGBP1 confers resistance to bortezomib-mediated apoptosis. *PLOS ONE*, *6*(5), e20254. https://doi.org/10.1371/journal.pone.0020254

[9] Gao, X., Jiang, L., Gong, Y., Chen, X., Ying, M., Zhu, H., . . . , & Cao, J. (2019). Stress granule: A promising target for cancer treatment. *British Journal of Pharmacology*, *176*(23), 4421–4433. https://doi.org/10.1111/bph.14790

[10] Reineke, L. C., & Neilson, J. R. (2019). Differences between acute and chronic stress granules, and how these differences may impact function in human disease. *Biochemical Pharmacology*, *162*, 123–131. https://doi.org/10.1016/j.bcp.2018.10.009

[11] Baghban, R., Roshangar, L., Jahanban-Esfahlan, R., Seidi, K., Ebrahimi-Kalan, A., Jaymand, M., . . . , & Zare, P. (2020). Tumor microenvironment complexity and therapeutic implications at a glance. *Cell Communication and Signaling*, *18*(1), 59. https://doi.org/10.1186/s12964-020-0530-4

[12] Leinonen, R., Sugawara, H., & Shumway, M. (2010). The sequence read archive. *Nucleic Acids Research*, *39*, D19–D21. https://doi.org/10.1093/nar/gkq1019

[13] Dobin, A., Davis, C. A., Schlesinger, F., Drenkow, J., Zaleski, C., Jha, S., . . . , & Gingeras, T. R. (2013). STAR: Ultrafast universal RNA-seq aligner. *Bioinformatics*, *29*(1), 15–21. https://doi.org/10.1093/bioinformatics/bts635

[14] Wingett, S. W., & Andrews, S. (2018). FastQ screen: A tool for multi-genome mapping and quality control. *F1000Research*, *7*, 1338. https://doi.org/10.12688/f1000research.15931.2

[15] Ewels, P., Magnusson, M., Lundin, S., & Käller, M. (2016). MultiQC: Summarize analysis results for multiple tools and samples in a single report. *Bioinformatics*, *32*(19), 3047–3048. https://doi.org/10.1093/bioinformatics/btw354

[16] Wang, L., Wang, S., & Li, W. (2012). RSeQC: Quality control of RNA-seq experiments. *Bioinformatics*, *28*(16), 2184–2185. https://doi.org/10.1093/bioinformatics/bts356

[17] Liao, Y., Smyth, G. K., & Shi, W. (2014). featureCounts: An efficient general purpose program for assigning sequence reads to genomic features. *Bioinformatics*, *30*(7), 923–930. https://doi.org/10.1093/bioinformatics/btt656

[18] Love, M. I., Huber, W., & Anders, S. (2014). Moderated estimation of fold change and dispersion for RNA-seq data with DESeq2. *Genome Biology*, *15*, 1–21. https://doi.org/10.1186/s13059-014-0550-8

[19] The Galaxy Community (2022). The Galaxy platform for accessible, reproducible and collaborative biomedical analyses: 2022 update. *Nucleic Acids Research*, *50*(W1), W345–W351. https://doi.org/10.1093/nar/gkac247

[20] Barrett, T., Wilhite, S. E., Ledoux, P., Evangelista, C., Kim, I. F., Tomashevsky, M., . . . , & Soboleva, A. (2012). NCBI GEO: Archive for functional genomics data sets—Update. *Nucleic Acids Research*, *41*(D1), D991–D995. https://doi.org/10.1093/nar/gks1193

[21] Luo, W., Pant, G., Bhavnasi, Y. K., Blanchard Jr, S. G., & Brouwer, C. (2017). Pathview Web: User friendly pathway

visualization and data integration. *Nucleic Acids Research*, *45*(W1), W501–W508. https://doi.org/10.1093/nar/gkx372

[22] Alhamdoosh, M., Ng, M., Wilson, N. J., Sheridan, J. M., Huynh, H., Wilson, M. J., & Ritchie, M. E. (2017). Combining multiple tools outperforms individual methods in gene set enrichment analyses. *Bioinformatics*, *33*(3), 414–424. https://doi.org/10.1093/bioinformatics/btw623

[23] Young, M. D., Wakefield, M. J., Smyth, G. K., & Oshlack, A. (2010). Gene ontology analysis for RNA-seq: Accounting for selection bias. *Genome Biology*, *11*, 1–12. https://doi.org/10.1186/gb-2010-11-2-r14

[24] Zhang, J., Zhang, Q., Zhang, J., & Wang, Q. (2020). Expression of ACAP1 is associated with tumor immune infiltration and clinical outcome of ovarian cancer. *DNA and Cell Biology*, *39*(9), 1545–1557. https://doi.org/10.1089/dna.2020.5596

[25] Li, S., Shi, X., Chen, M., Xu, N., Sun, D., Bai, R., . . . , & Xu, Z. (2019). Angiogenin promotes colorectal cancer metastasis *via* tiRNA production. *International Journal of Cancer*, *145*(5), 1395–1407. https://doi.org/10.1002/ijc.32245

[26] Yang, X., Cao, X., & Zhu, Q. (2025). p62/SQSTM1 in cancer: phenomena, mechanisms, and regulation in DNA damage repair. *Cancer and Metastasis Reviews*, *44*(1), 33. https://doi.org/10.1007/s10555-025-10250-w

[27] Frietze, K. K., Brown, A. M., Das, D., Franks, R. G., Cunningham, J. L., Hayward, M., & Nickels Jr, J. T. (2022). Lipotoxicity reduces DDX58/Rig-1 expression and activity leading to impaired autophagy and cell death. *Autophagy*, *18*(1), 142–160. https://doi.org/10.1080/15548627.2021.1920818

[28] Chaudhari, P. R., Charles, S. E., D'Souza, Z. C., & Vaidya, M. M. (2017). Hemidesmosomal linker proteins regulate cell motility, invasion and tumorigenicity in oral squamous cell carcinoma derived cells. *Experimental Cell Research*, *360*(2), 125–137. https://doi.org/10.1016/j.yexcr.2017.08.034

[29] Shen, Y., Sun, Y., Zhang, L., & Liu, H. (2017). Effects of DTX3L on the cell proliferation, adhesion, and drug resistance of multiple myeloma cells. *Tumor Biology*, *39*(6), 1010428317703941. https://doi.org/10.1177/1010428317703941

[30] Xu, P., Tao, X., Zhao, C., Huang, Q., Chang, H., Ban, N., . . . , & Wang, D. (2017). DTX3L is upregulated in glioma and is associated with glioma progression. *International Journal of Molecular Medicine*, *40*(2), 491–498. https://doi.org/10.3892/ijmm.2017.3023

[31] Hu, W., Hu, Y., Pei, Y., Li, R., Xu, F., Chi, X., . . . , & Yang, C. (2023). Silencing DTX3L inhibits the progression of cervical carcinoma by regulating PI3K/AKT/mTOR signaling pathway. *International Journal of Molecular Sciences*, *24*(1), 861. https://doi.org/10.3390/ijms24010861

[32] Wang, L., Sun, X., He, J., & Liu, Z. (2021). Functions and molecular mechanisms of deltex family ubiquitin E3 ligases in development and disease. *Frontiers in Cell and Developmental Biology*, *9*, 706997. https://doi.org/10.3389/fcell.2021.706997

[33] Gotovac, J. R., Liu, D. S. H., Yates, M. J., Milne, J. V., Macpherson, A. A., Simpson, K. J., . . . , & Clemons, N. J. (2020). GRB7 is an oncogenic driver and potential therapeutic target in oesophageal adenocarcinoma. *The Journal of Pathology*, *252*(3), 317–329. https://doi.org/10.1002/path.5528

[34] Tsai, N. P., Ho, P. C., & Wei, L. N. (2008). Regulation of stress granule dynamics by Grb7 and FAK signalling pathway. *The EMBO Journal*, *27*(5), 715–726. https://doi.org/10.1038/emboj.2008.19

[35] Xu, Q., Liu, Z., Zhu, Z. Q., Fan, Y., Chen, R., Xie, X. H., & Cheng, M. (2021). Knockdown of growth factor receptor bound protein 7 suppresses angiogenesis by inhibiting the secretion of vascular endothelial growth factor A in ovarian cancer cells. *Bioengineered*, *12*(2), 12179–12190. https://doi.org/10.1080/21655979.2021.2005225

[36] Mancarella, C., & Scotlandi, K. (2020). IGF2BP3 from physiology to cancer: Novel discoveries, unsolved issues, and future perspectives. *Frontiers in Cell and Developmental Biology*, *7*, 363. https://doi.org/10.3389/fcell.2019.00363

[37] Saadh, M. J., Ghnim, Z. S., Mahdi, M. S., Mandaliya, V., Ballal, S., Bareja, L., . . . , & Hamad, A. K. (2025). The emerging role of kinesin superfamily proteins in Wnt/β-catenin signaling: implications for cancer. *Pathology-Research and Practice*, 155904. https://doi.org/10.1016/j.prp.2025.155904

[38] Sim, C. K., Lee, J. H., Baek, I. J., Lee, S. W., & Lee, M. S. (2019). Enhanced antitumor immune response in 2'-5' Oligoadenylate Synthetase-Like 1-(OASL1-) deficient mice upon Cisplatin chemotherapy and radiotherapy. *Journal of Immunology Research*, *2019*(1), 7596786. https://doi.org/10.1155/2019/7596786

[39] Niepel, M., Vasbinder, M., Molina, J., Gui, B., Kunii, K., Blackwell, D., . . . , & Keilhack, H. (2022). The PARP14 inhibitor RBN-3143 suppresses lung inflammation in preclinical models. *European Respiratory Journal*, *60*, 4642. https://doi.org/10.1183/13993003.congress-2022.4642

[40] Bai, Y., Dong, Z., Shang, Q., Zhao, H., Wang, L., Guo, C., . . . , & Wang, Q. (2016). Pdcd4 is involved in the formation of stress granule in response to oxidized low-density lipoprotein or high-fat diet. *PLoS One*, *11*(7), e0159568. https://doi.org/10.1371/journal.pone.0159568

[41] Kubala, M. H., & DeClerck, Y. A. (2019). The plasminogen activator inhibitor-1 paradox in cancer: a mechanistic understanding. *Cancer and Metastasis Reviews*, *38*(3), 483–492. https://doi.org/10.1007/s10555-019-09806-4

[42] Damale, M. G., Pathan, S. K., Shinde, D. B., Patil, R. H., Arote, R. B., & Sangshetti, J. N. (2020). Insights of tankyrases: A novel target for drug discovery. *European Journal of Medicinal Chemistry*, *207*, 112712. https://doi.org/10.1016/j.ejmech.2020.112712

[43] Yi, Z., Arvola, R. M., Myers, S., Dilsavor, C. N., Abu Alhasan, R., Carter, B. N., . . . , & Singh, G. (2022). Mammalian UPF3A and UPF3B can activate nonsense-mediated mRNA decay independently of their exon junction complex binding. *The EMBO Journal*, *41*(10), e109202. https://doi.org/10.15252/embj.2021109202

[44] Karimian, A., Mir, S. M., Parsian, H., Refieyan, S., Mirza-Aghazadeh-Attari, M., Yousefi, B., & Majidinia, M. (2019). Crosstalk between phosphoinositide 3-kinase/Akt signaling pathway with DNA damage response and oxidative stress in cancer. *Journal of Cellular Biochemistry*, *120*(6), 10248–10272. https://doi.org/10.1002/jcb.28309

[45] Hu, X., Li, J., Fu, M., Zhao, X., & Wang, W. (2021). The JAK/STAT signaling pathway: From bench to clinic. *Signal Transduction and Targeted Therapy*, *6*(1), 402. https://doi.org/10.1038/s41392-021-00791-1

[46] Hu, Q., Bian, Q., Rong, D., Wang, L., Song, J., Huang, H., Zeng, J., Mei, J., & Wang, P. (2023). JAK/STAT pathway: Extracellular signals, diseases, immunity, and therapeutic regimens. *Frontiers in Bioengineering and Biotechnology*, *11*, 1110765. https://doi.org/10.3389/fbioe.2023.1110765

[47] Xu, J., Lin, H., Wu, G., Zhu, M., & Li, M. (2021). IL-6/STAT3 Is a Promising Therapeutic Target for Hepatocellular Carcinoma. *Frontiers in Oncology*, *11*, 760971. https://doi.org/10.3389/fonc.2021.760971

[48] Ribatti, D., Tamma, R., & Annese, T. (2020). Epithelial-mesenchymal transition in cancer: A historical overview. *Translational Oncology*, *13*(6), 100773. https://doi.org/10.1016/j.tranon.2020.100773

How to Cite: Jangid, V., Rahul, C. N., Rashmi B, A., & Sekar, K. (2024). Computational Analysis to Identify Novel Drug Targets for Esophageal Cancer. *Medinformatics*. https://doi.org/10.47852/bonviewMEDIN42023732

Abbreviations

SGs	Stress Granules
PI3K	Phosphoinositol-3-kinase
mTOR	Mammalian target of rapamycin
AC	Adenocarcinoma
Sec	Squamous cell carcinoma
GERD	Gastroesophageal reflux disease
FoxO	Fork-head box transcription factors
ROS	Reducing reactive oxygen
mRNA	Messenger Ribonucleic Acid
RBPs	RNA-Binding Proteins
ER	Endoplasmic reticulum
RNA-seq	RNA sequencing
GEO	Gene Expression Omnibus
SRA	Short Read Archive
NCBI	National Center for Biotechnology Information
QC	Quality Check
STAR	Spliced Transcripts Alignment to a Reference
RSeQC	RNA-seq data Quality Check
BAM	Binary Alignment Map
DESeq	Differential Expression Sequence
DEGs	Differentially expressed genes
logFC	Log fold change
PC	Principle Component
GO	Gene ontology
MF	Molecular function
BP	Biological processes
CC	Cellular component
KEGG	Kyoto Encyclopedia of Genes and Genomes
ERK	Extracellular signal-regulated kinases
JAK-STAT	Janus kinase/signal transducers and activators of transcription
MSGP	Mammalian Stress Granules Proteome
EMT	Epithelial-Mesenchymal Transition